

27p

Code 1
CR 56459

NG4-24039
cat 29

Technical Report No. 32-594

*An Evaluation of the Communication Blackout Problem
for a Blunt Mars-Entry Capsule
and a Potential Method for the Elimination of Blackout*

Dwain F. Spencer

001

125

jpl

JET PROPULSION LABORATORY
CALIFORNIA INSTITUTE OF TECHNOLOGY
PASADENA, CALIFORNIA

April 15, 1964


OTS PRICE

XEROX \$ 260^{ph}
MICROFILM \$ _____

Technical Report No. 32-594

*An Evaluation of the Communication Blackout Problem
for a Blunt Mars-Entry Capsule
and a Potential Method for the Elimination of Blackout*

Dwain F. Spencer


for Charles W. Cole, Chief
Engineering Mechanics Division

JET PROPULSION LABORATORY
CALIFORNIA INSTITUTE OF TECHNOLOGY
PASADENA, CALIFORNIA

April 15, 1964

Copyright © 1964
Jet Propulsion Laboratory
California Institute of Technology

Prepared Under Contract No. NAS 7-100
National Aeronautics & Space Administration

CONTENTS

I. Introduction	1
II. Plasma Attenuation of a Transmitted Signal	2
III. Characteristics of the Martian Atmosphere and the Capsule Entry Trajectory	3
IV. Electron Concentration in the Vicinity of the Mars-Entry Capsule	5
V. Extension of Results to Other Entry Conditions and Atmospheric Models	9
VI. Capsule Instrumentation as an Entry Failure Contingency	12
VII. Other Considerations in the Flow Field and Methods of Eliminating Blackout	13
VIII. Conclusions	18
Nomenclature	18
References	19
Bibliography	21

TABLE

1. Stagnation-region values of C , i , and j for a Mars-entry capsule	12
---	----

FIGURES

1. Attenuation of a 2295-Mc signal versus plasma electron concentration for a collisionless plasma	2
2. Mars-entry trajectory	4
3. Capsule velocity versus altitude at Mars for $V_E = 26,600$ fps and a capsule $m/C_D A = 0.2$ slug/ft ²	4
4. Capsule altitude versus time from entry at 200 km for $V_E = 26,600$ fps and a capsule $m/C_D A = 0.2$ slug/ft ²	4

FIGURES (Cont'd)

5. Electron concentration versus capsule altitude for $\psi_E = 90$ deg	6
6. Electron concentration versus capsule altitude for $\psi_E = 20$ deg	6
7. Entry capsule with fluid-injection system	7
8. Mollier diagram for a Martian atmospheric composition of 40 percent N_2 , 30 percent CO_2 , and 30 percent A	7
9. Gas and electron collision frequencies in the stagnation and wake regions versus capsule altitude	8
10. Maximum plasma frequency in the wake of a Mars-entry body (based on an isentropic frozen expansion to P_∞)	9
11. Electron concentration versus time from entry for various entry velocities and for $\psi_E = 90$ deg	10
12. Electron concentration versus time from entry for various entry velocities and for $\psi_E = 20$ deg	10
13. Blackout duration versus entry velocity	10
14. Profiles for deceleration and for convective and radiative heat-transfer rates during entry for $\psi_E = 90$ deg	12
15. Profiles for deceleration and for convective and radiative heat-transfer rates during entry for $\psi_E = 20$ deg	12
16. Estimate of electron depletion resulting from recombination for $\psi_E = 90$ deg	14
17. Estimated flow rate of CCl_4 necessary to eliminate blackout during Mars entry for $V_E = 26,600$ fps, $m/C_D A = 0.2$ slug/ft ² , and $\psi_E = 90$ deg	16
18. Relative importance of atomic and electron collisions in CCl_4 dissociation	17

ABSTRACT

24039

Unless preventive methods are utilized, it appears that the communications link from a blunt body entering the Martian atmosphere will be blacked out during entry because of the free electron concentration in the wake of the capsule. Estimates of the free electron concentration in the wake indicate peak values of approximately 3×10^{12} electrons/cm³, whereas the critical electron concentration for S-band transmission at 2295 Mc is 10^{11} electrons/cm³. The injection of a high-electron-affinity fluid such as carbon tetrachloride may reduce the free electron concentration below this critical value. The amount of fluid required is estimated to be on the order of 1-10 lb. The latter statement must be experimentally confirmed, however, before the use of an auxiliary fluid-injection system can be fully evaluated. *Author*

I. INTRODUCTION

The acquisition of data from a capsule entering a planetary atmosphere is dependent upon the ability of the communications system to transmit the physical data to Earth. This requirement is dependent not only on the ability of the electronics of the communications system to function properly, but also on the ability of the Earth-based receiver to acquire and to retain the signal transmitted from the entry capsule. The transmitted signal may fail to arrive at the receiver because of (1) the dynamics of the entering capsule, (2) the electrons that may be present in the wake of the capsule, and/or (3) the Doppler shift in the signal as the capsule is decelerated during planetary entry. Although all three effects must be considered in order to determine the probability of

successfully obtaining the desired data during a planetary entry, this Report is restricted to an analysis of the blackout problem owing to ionization of the planetary atmosphere in the vicinity of the entry capsule.

One of the presently conceived designs for the *Mariner* Mars-entry capsule utilizes a direct communications link from the entry capsule to Earth. The transmission frequency for this link will be 2295 Mc (S band). Although many of the aspects of this Report are applicable to other planetary entry capsules, the specific results are limited to this transmission frequency and to the Martian atmosphere.

II. PLASMA ATTENUATION OF A TRANSMITTED SIGNAL

As is well known from Earth atmospheric entry flights, a plasma will surround an entering body in certain ranges of atmospheric density and capsule velocity. This plasma attenuates electromagnetic waves that may be incident upon it by absorption and reflection. For a plane electromagnetic wave penetrating a homogeneous plasma (Ref. 1 and 2), the propagation vector is dependent upon (1) the transmission frequency, (2) the electron collision frequency, and (3) the plasma frequency. The electron collision frequency represents the number of collisions per second of electrons with various species in the plasma and determines the degree of attenuation when the transmission frequency is greater than the plasma frequency. The plasma frequency is defined by

$$\omega_p^2 = \sum_{i=1}^I \left[\frac{n_i (Ze)_i^2}{m_i \epsilon_0} \right] \quad (1)$$

where the symbols are defined in the Nomenclature and the sum is over all of the ionized species present in the plasma. It is assumed that the plasma is electrically neutral, that is, that the number of electrons and negative ions present equals or is greater than the number of positive ions present. Since the mass of the electrons is at least three orders of magnitude less than that of the ions present, the plasma frequency is determined by the electron concentration, that is, by

$$\omega_p^2 \simeq \omega_{p,e}^2 = \frac{n_e e^2}{m_e \epsilon_0} \quad (2)$$

which may be expressed in cgs units as

$$\omega_p = 5.64 \times 10^4 n_e^{1/2} \quad (3)$$

Examination of the relation for the propagation vector leads to the definition of the critical plasma frequency, that is, the plasma frequency that corresponds to the transmission frequency:

$$(\omega_p)_{cr} = 2\pi f \quad (4)$$

where f is the transmission frequency in cycles per second. By utilizing Eq. (3) and (4), and the fact that $f = 2.295 \times 10^9$ cycles/sec, one can obtain the electron concentration that produces the critical plasma frequency. This critical value of the electron concentration is 6.5×10^{10} electrons/cm³.

As was discussed previously, the attenuation of the electromagnetic waves is dependent upon the electron collision frequency in the plasma, since the electrons are the principal contributors to reflection of waves in a plasma. However, for the gas densities and the capsule velocities of interest, since the collision frequency is much less than the critical plasma frequency, the collisional effects on wave propagation are not important, although collisions are important in determining the thermodynamic state of the gas. Lin (Ref. 3) shows that, in this case, the propagation constant can be factored into a real and an imaginary part. The extinction coefficient at wavelength λ is simply

$$k' = k'_\lambda = \left(\frac{\omega_{p,e}^2 - \omega^2}{\omega^2} \right)^{1/2} \quad (5)$$

where k' is real. Thus the electromagnetic wave is attenuated (by dispersion) for $\omega_p > \omega$ and is unaffected for $\omega_p < \omega$.¹ Since the collision frequency has, in fact, a nonzero value, there will be some attenuation when $\omega > \omega_p$; as will be shown later, however, the effect of

¹The extinction coefficient k'_λ , defined by Lin, is equal to $-i\lambda\kappa/2\pi$ in the standard literature. The propagation constant, therefore, is given by $|\kappa| = 2\pi k'_\lambda/\lambda$. The real solution for k'_λ corresponds to the pure imaginary solution for the propagation constant κ , that is, when $\omega_p > \omega$. The imaginary solution for k'_λ corresponds to the real solution for κ'_λ , that is, when $\omega > \omega_p$.

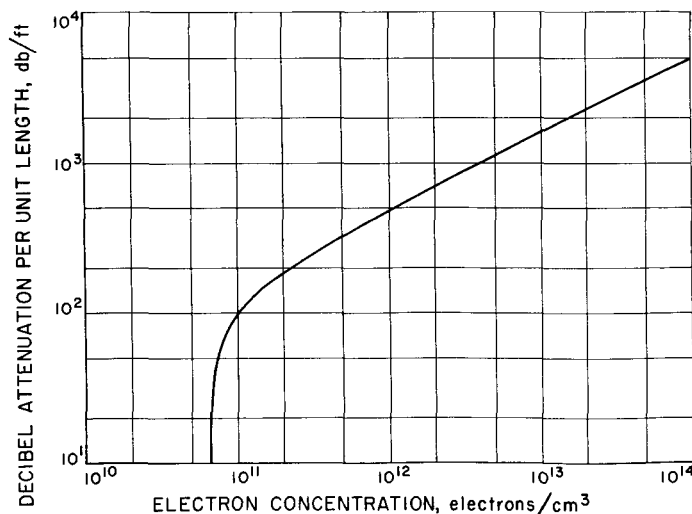


Fig. 1. Attenuation of a 2295-Mc signal versus plasma electron concentration for a collisionless plasma

this attenuation is negligible. The total attenuation of the transmitted signal is determined by the attenuation coefficient and by the depth of plasma that the wave must penetrate. The decibel attenuation is given by

$$\text{db attenuation} = 20 \log_{10} \left| \frac{E_0}{E} \right| \quad (6)$$

For a plane monochromatic wave traveling through a plasma of thickness z_p , the attenuation is

$$\left| \frac{E_0}{E} \right| = \exp \left[\int_0^{z_p} \kappa(\lambda, z) dz \right] = \exp \left[\frac{2\pi}{\lambda} \int_0^{z_p} k'_\lambda(z) dz \right] \quad (7)$$

and

$$\text{db attenuation} = \frac{54.6}{\lambda} \bar{k}'_\lambda z_p \quad (8)$$

The decibel attenuation per unit length for a 2295-Mc signal is given in Fig. 1, where it is plotted versus electron concentration in a collisionless plasma. The signal attenuation² increases very rapidly for electron concentrations $\geq 6.5 \times 10^{10}$ electrons/cm³ and is approximately 100 db/ft at an electron concentration of 10^{11} electrons/cm³. Thus, the signal is assumed to be lost if it must penetrate a plasma with an electron concentration greater than 10^{11} electrons/cm³.

²The attenuation is expressed in decibels per foot, since the characteristic dimension of the *Mariner* entry capsule is expressed in feet.

III. CHARACTERISTICS OF THE MARTIAN ATMOSPHERE AND THE CAPSULE ENTRY TRAJECTORY

At present, there is substantial uncertainty regarding the values of the physical properties of the Martian atmosphere and the variation of these properties with altitude above the Martian surface. In order to provide an expected worst case (from the standpoint of available time for the communication of data to Earth), a model atmosphere based on Kaplan's recent findings (Ref. 4) has been assumed. The surface pressure is assumed to be 11 mb (23 lb/ft²), and the atmosphere is assumed to be isothermal at a temperature of 180°K. Based on these assumptions, the surface density is 2.5×10^{-5} g/cm³ (4.8×10^{-5} slug/ft³). An atmospheric composition of 40 percent N₂, 30 percent CO₂, and 30 percent A is adopted as a nominal composition. These assumptions result in a scale height β of 0.092 km⁻¹ (2.8×10^{-5} ft⁻¹).

Since the atmosphere is assumed to be isothermal, density and static pressure each follow an exponential decay law with altitude of the form

$$\rho = \rho_s e^{-\beta h} \quad (9)$$

$$P = P_s e^{-\beta h} \quad (10)$$

A discussion of the consequences of different assumptions regarding surface pressure (density) and composition is presented in Section V.

In order to simplify the analysis, a straight-line trajectory is assumed during entry at a constant angle relative

to the local horizontal ψ . The surface of Mars is assumed to be flat so that the altitude above the surface at any time is independent of the ground range from the assumed point of entry into the atmosphere (Fig. 2). For an entry angle ψ_E of 90 deg, the solution is exact (neglecting the rotation of Mars); at an entry angle of 20 deg, however, the curvature of Mars is no longer negligible in determining the velocity-time (altitude) history of the capsule. However, for purposes of estimating the potential blackout problem, this consideration should merely shift the electron profile to some later time but should not substantially change the absolute value of the blackout time.

With these simplifying assumptions, the velocity-altitude and time-altitude variations for a ballistic entry (Ref. 5 and 6) are given by

$$V = V_E \exp \left[\frac{-P}{2g_m \Delta \sin \psi_E} \right] \quad (11)$$

$$t_t - t_E = \frac{1}{\beta V_E \sin \psi_E} \left[\bar{E}_i \left(\frac{P_t}{2g_m \Delta \sin \psi_E} \right) - \bar{E}_i \left(\frac{P_E}{2g_m \Delta \sin \psi_E} \right) \right] \quad (12)$$

where

$$\bar{E}_i(\zeta) = \int_{-\infty}^{\zeta} \frac{e^u}{u} du$$

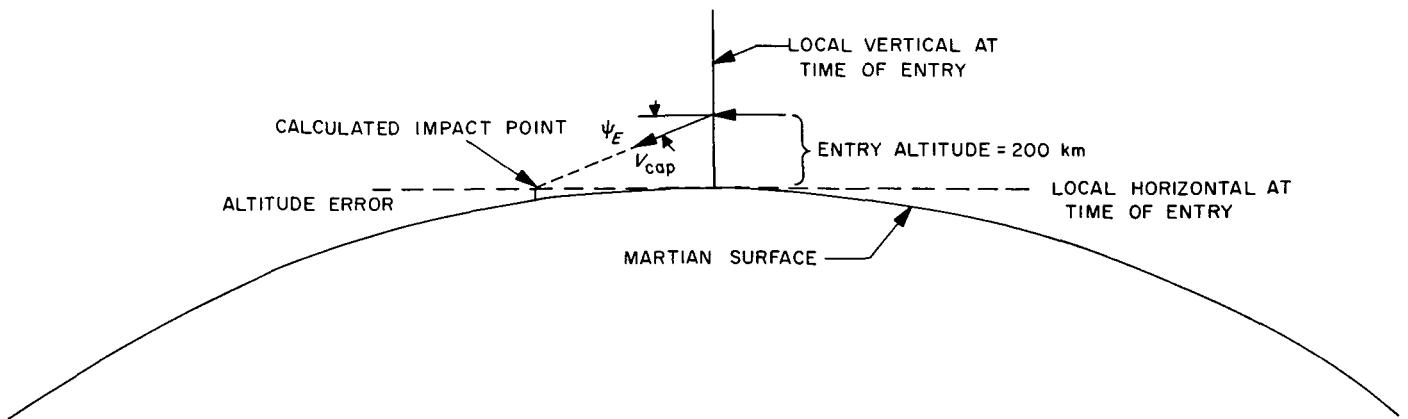


Fig. 2. Mars-entry trajectory

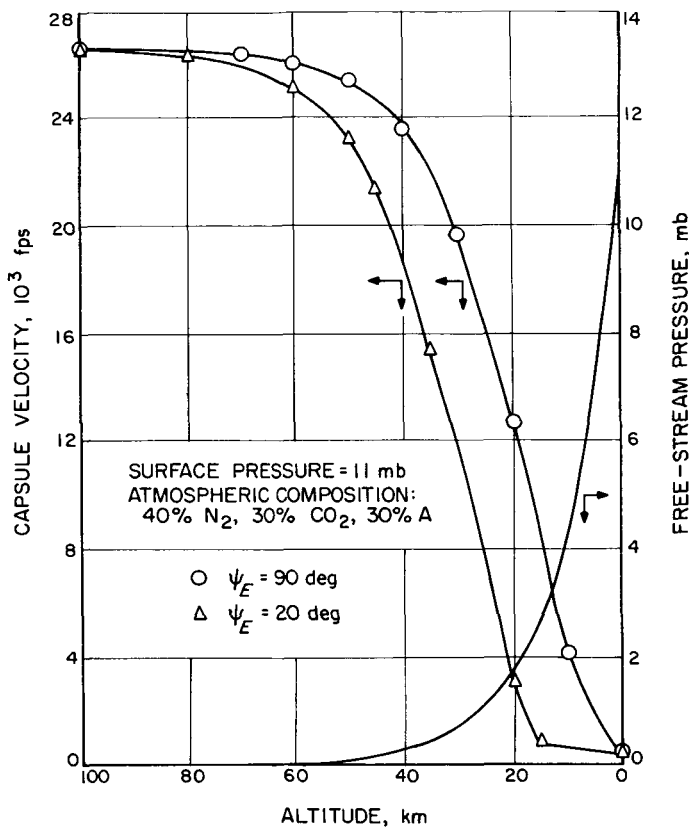


Fig. 3. Capsule velocity versus altitude at Mars for
 $V_E = 26,600$ fps and a capsule
 $m/C_D A = 0.2$ slug/ft²

Figures 3 and 4 are obtained from Eq. (10), (11), and (12) for an entry velocity of 26,600 fps, for entry angles of 90 and 20 deg, and for a ballistic coefficient of 0.2 slug/ft². This value of the ballistic coefficient is necessary in order to obtain sufficient braking at high altitudes in the tenuous Martian atmosphere. The entry velocity

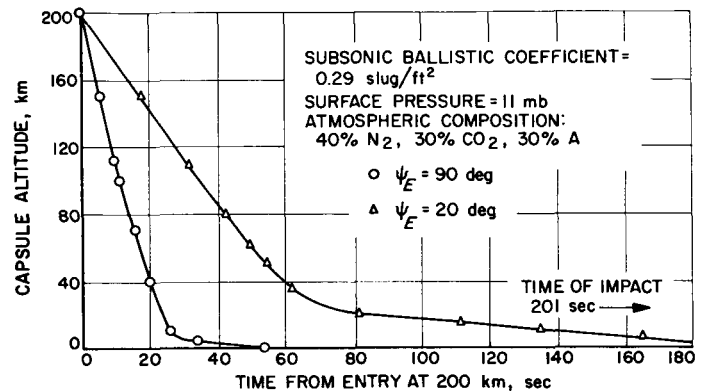


Fig. 4. Capsule altitude versus time from entry at 200 km
for $V_E = 26,600$ fps and a capsule
 $m/C_D A = 0.2$ slug/ft²

of 26,600 fps was selected since it represents an expected worst-case entry condition for the Mars oppositions in 1967, 1969, and 1971.

As pointed out in Ref. 5, the principal characteristics of interest in ballistic entry can be put in the form

$$F = C \rho^i V^j \quad (13)$$

where i and j are the exponents of the density and the velocity dependence, respectively. From this relationship, one may obtain relatively simple profiles for the parameters that may be empirically fit to this form, for example, capsule deceleration and stagnation heating rates. The simplicity of this relation suggests that an empirical fit of *calculated* electron concentrations in this form would be useful. A fit to the capsule data for the Mars entry is discussed below.

IV. ELECTRON CONCENTRATION IN THE VICINITY OF THE MARS-ENTRY CAPSULE

The exact analysis of the electron concentration in the vicinity of the Mars-entry capsule is quite complex because of nonequilibrium effects. For example, the production of electrons is dependent on the time required for equipartition of the translational energy of the gas in the bow shock and on the residence time of the gas in the stagnation region. The electron concentration aft of the entry capsule is not only dependent on the rate of production of electrons, but also on the relaxation rate of the gas in the flow past the body. In general, since there is considerable uncertainty regarding the values of the relaxation rates, the evaluation of the local gas properties is difficult.

This analysis utilizes an approximate solution based on chemical equilibrium in the stagnation region of the entry capsule, and the analysis is strictly applicable only for altitudes of less than 100 km at Mars. This limit is determined by the entry body diameter, which is here assumed to be 10 ft, and by the Martian density profile discussed above. At altitudes greater than 100 km, the flow can no longer be considered to be in equilibrium, and the Rankine-Hugoniot relations across the shock are no longer valid (Ref. 7). It is felt, however, that an equilibrium solution at higher altitudes produces a conservative estimate of the degree of ionization; thus the results have been extrapolated to higher altitudes.

The equilibrium electron concentration in the stagnation region of the capsule is determined from an equilibrium thermochemistry and normal-shock program developed by T. Horton of the Jet Propulsion Laboratory (JPL). The program includes an evaluation of the equilibrium thermodynamic state of the gas for specified free-stream conditions and for a particular shock velocity. An empirical fit to the calculated data of the form given in Eq. (13) has been made for the electron concentration. The approximate result is within 50 percent of the calculated value for shock velocities between 14,000 and 30,000 fps, with the fit biased to provide a conservative estimate for velocities above 22,000 fps, since this represents the principal range of interest. The empirical fit for the nominal atmosphere (40 percent N_2 , 30 percent CO_2 , 30 percent A) is

$$n_{e,0} = 4.9 \times 10^{-32} \rho^{0.95} V^{11.8} \quad (14)$$

where

$$(14,000 \text{ fps} \leq V \leq 30,000 \text{ fps})$$

By utilizing Eq. (14) in connection with Fig. 3 and with the assumed variations of density with altitude, the stagnation-region electron-concentration profile was developed for entry angles of 90 and 20 deg (Fig. 5 and 6). The maximum electron concentration in the stagnation region is much greater than the critical electron concentration of 10^{11} electrons/cm³ for either the 90- or 20-deg entry case; in fact, it would indicate blackout of a signal propagating through the stagnation region for altitudes in the range from 150 to 18 km. In the *Mariner* capsule design, however, the antenna is at the rear of the capsule and is not required to transmit through the stagnation region. Since the signal must pass through the wake of the capsule, as depicted in Fig. 7, it is necessary to determine the electron concentration in the wake.

Three methods have been utilized to estimate the electron concentration in the wake. The first is based on the assumption that the total number of electrons formed in the stagnation region is a constant (frozen flow) as the ionized gas flows past the body. The change in electron concentration is thus caused by expansion of the gas.

Although the isentropic expansion coefficient is not a constant during the gas expansion, the results are quite insensitive to the value selected (see Fig. 5). Thus, the electron concentration in the wake (rear face of entry capsule) is given by

$$n_{e,w} = n_{e,0} \left(\frac{P_\infty}{P_0} \right)^{1/\gamma} \quad (15)$$

The pressure ratio across the shock, P_0/P_∞ , can be obtained from the normal-shock solution for various entry conditions; it has been found, however, that the pressure ratio across the shock can be predicted to within 30 percent by employing the Rankine-Hugoniot relations for a normal shock with a constant isentropic expansion coefficient. Then

$$\frac{P_0}{P_\infty} = 1 + \frac{2\gamma (M_{\text{cap}}^2 - 1)}{\gamma + 1} \quad (16)$$

It should be noted that the prediction of density and temperature ratios from the simple Rankine-Hugoniot relations is not so accurate as the prediction of the pressure ratio.

Since the stagnation-region equilibrium electron concentration is known from the normal-shock program

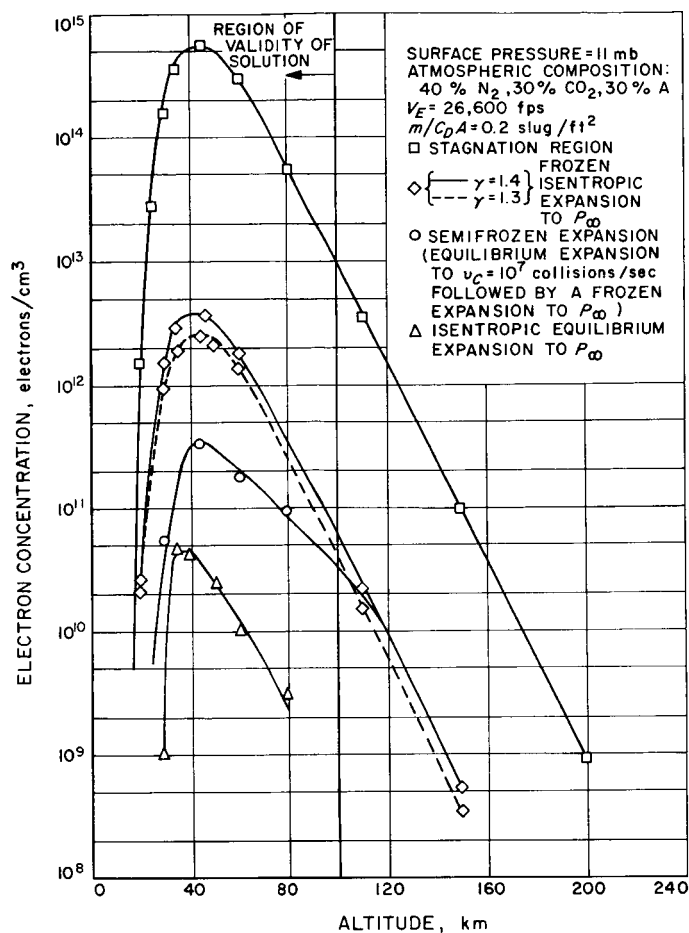


Fig. 5. Electron concentration versus capsule altitude
for $\psi_E = 90$ deg

results (or from the empirical fit of Eq. 14), the frozen-flow electron concentration in the wake can be obtained by combining Eq. (15) and (16). Frozen-flow electron concentrations in the wake are given for $\gamma = 1.3$ and $\gamma = 1.4$ in Fig. 5 and for $\gamma = 1.4$ in Fig. 6 for an entry velocity of 26,600 fps. The frozen-flow expansion reduces the maximum electron concentration by approximately two orders of magnitude and reduces the apparent blackout altitude to approximately 100 km.

The second method of estimating the electron concentration in the wake is based on the assumption that there is an isentropic equilibrium expansion of the gas from the stagnation pressure to the free-stream pressure. In order to evaluate numerically the conditions in the wake, a Mollier diagram for the 40 percent N₂, 30 percent CO₂,

³Isentropic expansion coefficients for various Mars atmospheric models range from 1.3 to 1.4.

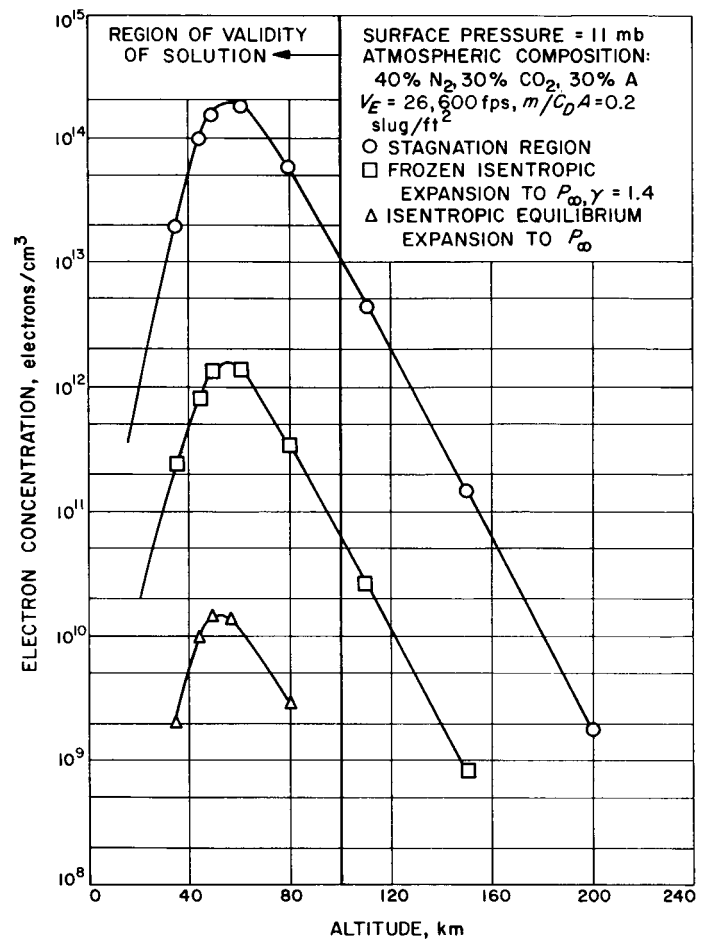


Fig. 6. Electron concentration versus capsule altitude
for $\psi_E = 20$ deg

30 percent A mixture was constructed (Fig. 8), using a subroutine of the thermochemistry program developed by T. Horton. The results of these calculations are also presented in Fig. 5 and 6 for an entry velocity of 26,600 fps. Based on an isentropic equilibrium expansion of the gas, one would not expect blackout to occur for entry velocities of less than 26,600 fps.

The final method employs a combination of equilibrium and frozen flow. Bray (Ref. 8) considered the case of flow through a rocket nozzle. He found that the flow could be considered to be in equilibrium to some cutoff point, at which the flow was frozen. As the chamber pressure of the rocket is decreased, Bray finds that the frozen-flow approximation throughout the nozzle becomes an increasingly better approximation to the actual flow conditions. An examination of his analysis indicates that the flow would be in equilibrium in a typical rocket engine for collision frequencies greater than 10^9

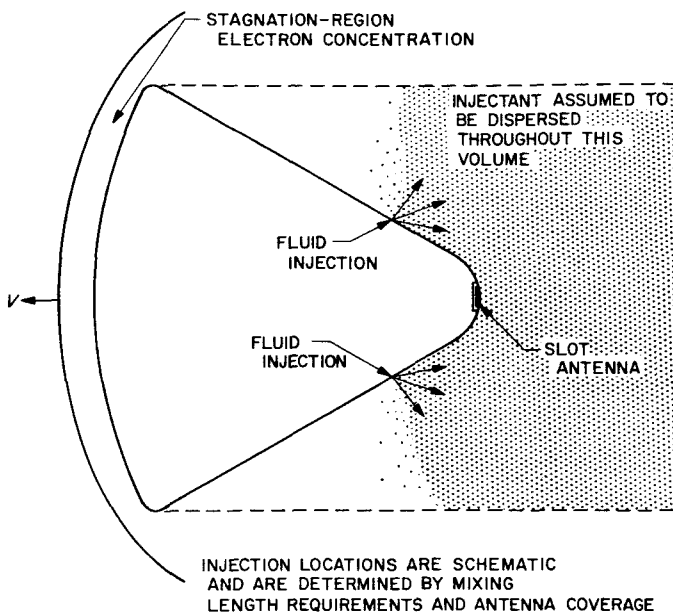


Fig. 7. Entry capsule with fluid-injection system

collisions/sec and frozen for lower collision frequencies. Since the residence time in a rocket nozzle is on the order of 10^{-4} sec, the average number of collisions per particle required for the flow to be in equilibrium in the nozzle is 10^5 .

If a similar argument is applied to the flow around the entry capsule, an *estimate* can be made of the state of the gas, that is, of the approach to equilibrium. At the temperatures present in the stagnation region of the entry capsule, the fraction of collisions that will cause a chemical reaction to occur will be greater than in a rocket nozzle since the kinetic temperature of the various species will be higher. Since activation energies for many chemical reactions are on the order of 1 eV, the collision efficiency is expected to be higher by approximately a factor of 20 in the stagnation region than in a rocket nozzle and higher by approximately a factor of 10 in the wake of the entry capsule than in a rocket nozzle. Since the residence time of the hot gas in flowing over the capsule is approximately 4×10^{-4} sec, a collision frequency of approximately 10^7 collisions/sec would be required for equilibrium based on the gas stagnation temperature, and 2×10^7 collisions/sec based on the estimated wake temperature. In order to *estimate* the approach to equilibrium, an average collision frequency in the gas of 10^7 collisions/sec is adopted as a requirement for equilibrium gas flow. At lower collision frequencies, the gas composition is assumed to be frozen.

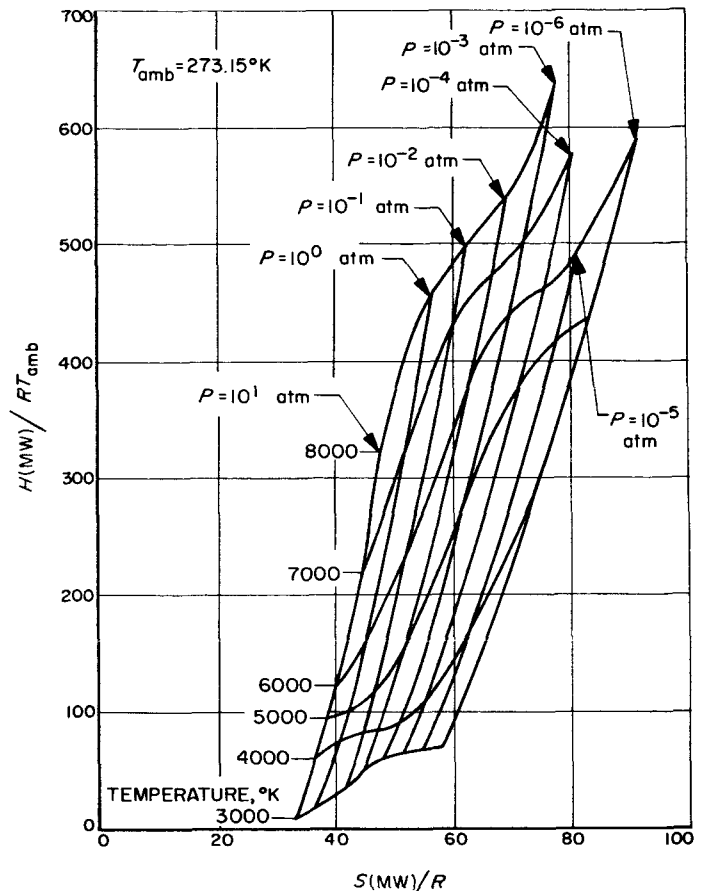


Fig. 8. Mollier diagram for a Martian atmospheric composition of 40 percent N_2 , 30 percent CO_2 , and 30 percent A

Now, the average particle collision frequency is given by

$$\bar{\nu}_i = \frac{\sum_{i=1}^I n_i v_i}{\sum_{i=1}^I n_i} \quad (17)$$

where the summation is over all molecular, atomic, and ionic species. The average collision frequency as determined from Eq. (17) has been evaluated along the 90-deg entry trajectory in the stagnation and wake regions, using average cross section data for all atomic and molecular species from Fay and Kemp (Ref. 9). The cross section for electron-ion, ion-ion, or electron-electron collisions is estimated by assuming binary collisions associated with long-range Coulomb forces. From Ref. 10, the cross section is given by

$$Q = \frac{\pi e^4}{(kT)^2} \quad (18)$$

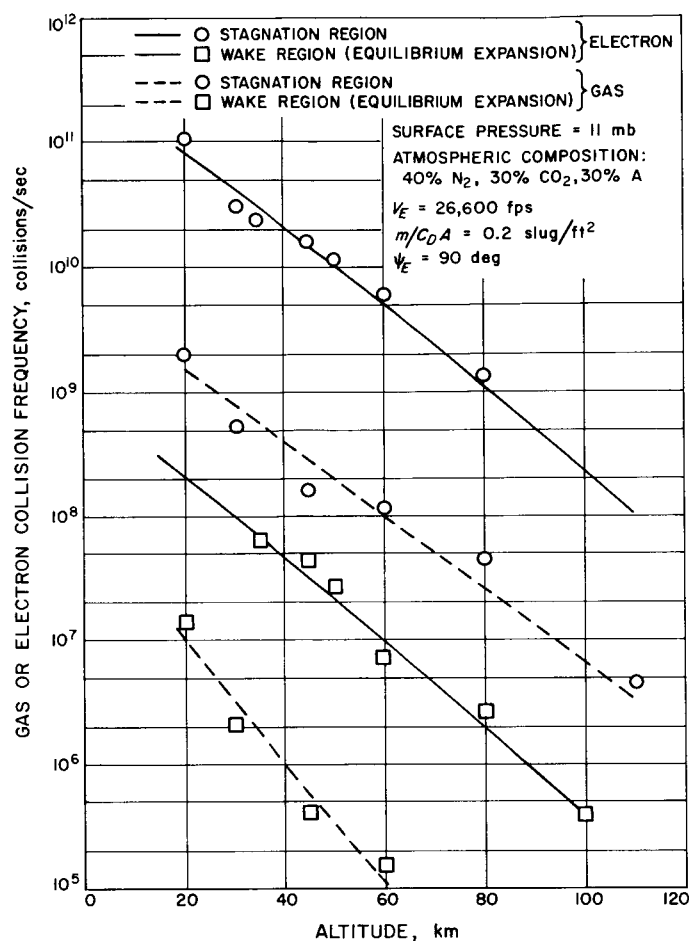


Fig. 9. Gas and electron collision frequencies in the stagnation and wake regions versus capsule altitude

The average collision frequency in the stagnation and wake regions is shown in Fig. 9. It is expected that the gas in the stagnation region will be in equilibrium for altitudes in the nominal Martian atmosphere of less than 100 km. This is in excellent agreement with the estimated threshold altitude for continuum flow theory. It is not

expected, however, that the wake will be in equilibrium for altitudes greater than approximately 20 km.

In order to evaluate the electron concentration in the wake as a function of altitude, it is assumed that the gas envelope around the entry body is in equilibrium for collision frequencies greater than 10^7 collisions per second and is frozen for lower collision frequencies. The gas was assumed to undergo an equilibrium expansion from the stagnation region to an average collision frequency of 10^7 collisions per second (using the Mollier diagram), followed by a frozen expansion to ambient pressure (semi-frozen expansion). The resulting electron-concentration profile is shown in Fig. 5 for a 90-deg entry angle. The calculations indicate that blackout would be expected to occur over the altitude range from 80 to 33 km. The results also indicate that the frozen-flow approximation yields a conservative estimate of the blackout time interval; therefore, in the following discussion, *the blackout time interval is assumed to be that corresponding to the all-frozen-flow case unless otherwise noted.*

Before the importance of the blackout time interval is discussed, the effect of the finite electron collision frequency on the electromagnetic wave attenuation coefficient must be examined. The estimated electron collision frequency in the stagnation and wake regions is shown in Fig. 9. When the plasma frequency is much greater than the electron collision frequency in the wake ($\approx 10^{11}$ compared to $\approx 10^8$), there will be little effect of collisions for $\omega_p < \omega$ (Ref. 2 and 3). At the high-altitude cutoff, the plasma frequency in the wake is approximately 10^{10} rad/sec, and the electron collision frequency is very low ($\approx 10^6$ collisions/sec); thus one would not expect any attenuation owing to collisions at high altitudes. An estimate of the attenuation at low altitudes (30 km, $\nu_w = 10^8$ collisions/sec, $\omega_p = 10^{10}$ rad/sec) shows the attenuation to be approximately 1 db/ft. Thus the blackout region will not be extended significantly to lower altitudes when collisional effects are included.

V. EXTENSION OF RESULTS TO OTHER ENTRY CONDITIONS AND ATMOSPHERIC MODELS

If it is assumed that the blackout time can be conservatively estimated by considering the frozen-flow analysis (see previous discussion), the electron concentration in the wake for other entry velocities can be calculated. By utilizing Eq. (14), (15), and (16), with $M^2 \gg 1$, the electron concentration in the wake is given by

$$n_{e,w} = 6.36 \times 10^{-28} \rho^{0.95} V^{10.37} \quad (19)$$

$$14,000 \text{ fps} \leq V \leq 30,000 \text{ fps}$$

Now for an isothermal atmosphere, the velocity profile is independent of the entry velocity; thus the same fractional velocity is attained at a particular altitude, independent of the entry velocity. Since this condition implies that the free-stream density is the same, the same electron concentration profile will be obtained. Now the electron concentration in the wake corresponding to any entry velocity other than that already considered (26,600 fps) is given by

$$(n_{e,w})_h^{V_E} = (n_{e,w})_h^{26,600} \left(\frac{V_E}{26,600} \right)^{10.37} \quad (20)$$

This equation holds, provided that the *local* capsule velocity satisfies the relation $14,000 \text{ fps} \leq V \leq 30,000 \text{ fps}$. By employing Eq. (3), the maximum plasma frequency in the wake versus entry velocity may be obtained. This is given in Fig. 10 for entry angles of 90 and 20 deg. Figure 10 shows that blackout would not be expected for entry velocities of less than 19,000 fps for a 90-deg entry angle or of less than approximately 21,000 fps for a 20-deg entry angle. Since these values are based on estimates of the electron concentration in the wake that are expected to be conservative, it appears that blackout could be eliminated by utilizing a retro propulsion maneuver prior to capsule entry.

By employing Eq. (20) for various entry velocities, the electron concentration versus time from entry at some altitude (200 km) can be obtained for various entry velocities. Electron concentration profiles and the anticipated duration of blackout are shown in Fig. 11 and 12 for various entry velocities. It should be recalled that blackout is initiated at the shorter time (left of Figure) and is terminated at a later time. The high-altitude cutoff, which has the greatest uncertainty associated with it, is thus to the left in Fig. 11 and 12. The blackout duration for each of the entry velocities is indicated in the Figures.

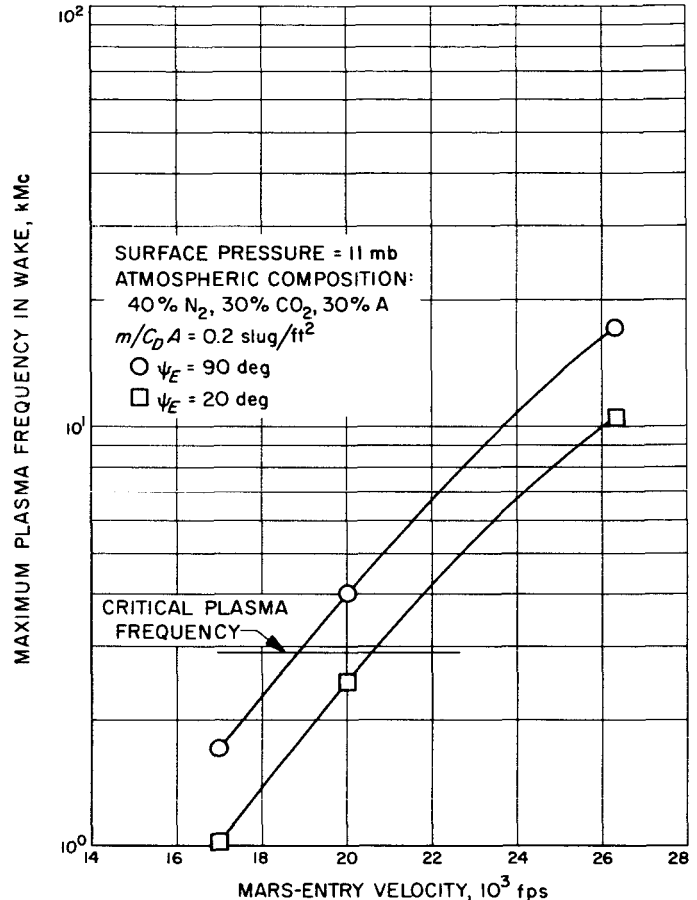


Fig. 10. Maximum plasma frequency in the wake of a Mars-entry body (based on an isentropic frozen expansion to P_∞)

These values of blackout duration can be utilized to obtain Fig. 13, which relates the blackout duration to entry velocity for $\psi_E = 90$ and 20 deg. As would be expected, the blackout duration is generally longer for the shallow entry angle; however, the time from end of blackout to impact is much greater for the shallow entry. For example, by utilizing Fig. 4 for $V_E = 26,600$ fps, the time from end of blackout to impact is 30 sec for a 90-deg entry angle and 135 sec for a 20-deg entry angle, assuming that there is no terminal parachute deployment.

The calculations in this Report have been carried out for a ballistic coefficient of 0.2 slug/ft²; however, the blackout time interval is not greatly affected by the ballistic coefficient. Basically, a reduction in the ballistic

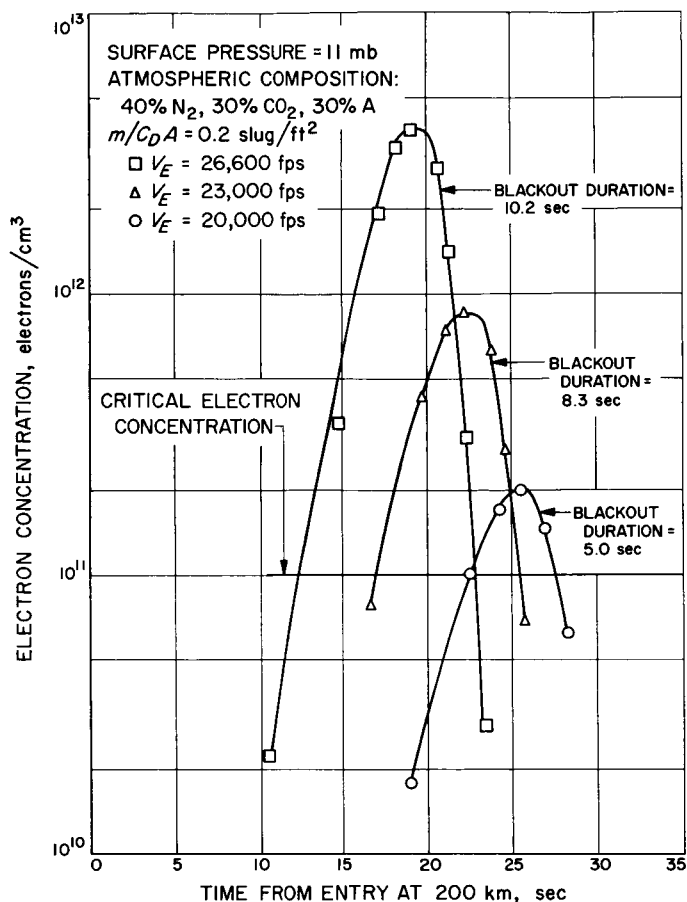


Fig. 11. Electron concentration versus time from entry for various entry velocities and for $\psi_E = 90^\circ$

coefficient results in a slightly lower electron concentration, since the velocity is less at a given altitude, that is, free-stream density. However, the electron concentration is much less dependent on density (proportional to $\rho^{0.95}$) than it is on velocity ($V^{10.4}$). Therefore, small variations (within a factor of two) in the ballistic coefficient would not be expected to produce significantly different results.

Scaling the electron concentration and blackout periods to other atmospheres is quite important because of the uncertainty in the value of the Martian atmospheric properties. For model atmospheres with different surface pressures (surface density) and the same composition as the nominal model atmosphere (atmosphere 1: 40 percent N₂, 30 percent CO₂, 30 percent A), the electron concentration profile can be shifted to the altitude at which the density is the same as that in the nominal atmosphere. This is possible since the scale height of each atmosphere is the same if both atmospheres are isothermal at the same temperature.

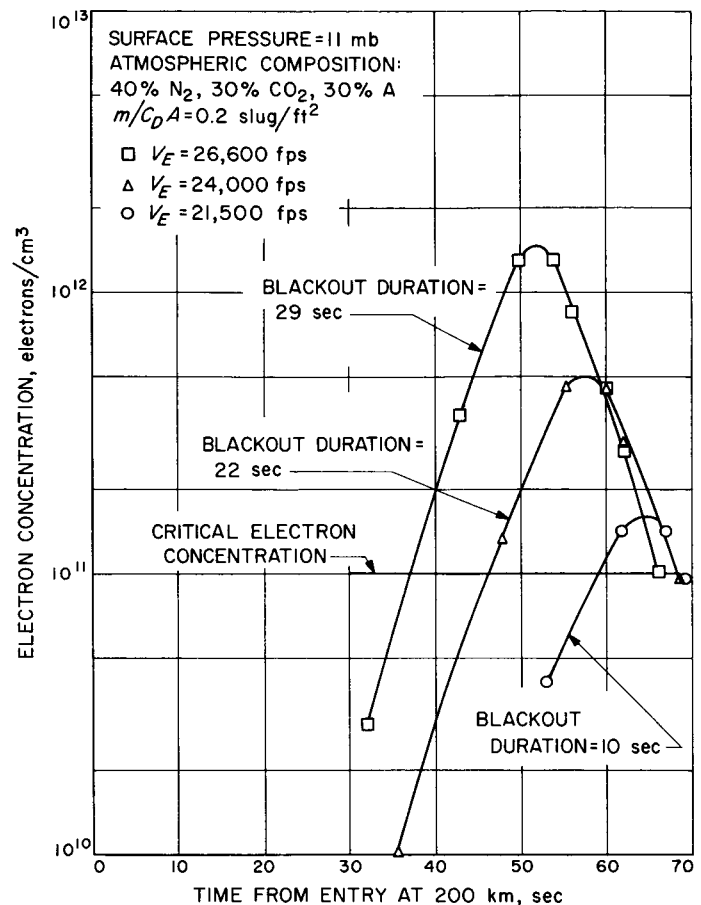


Fig. 12. Electron concentration versus time from entry for various entry velocities and for $\psi_E = 20^\circ$

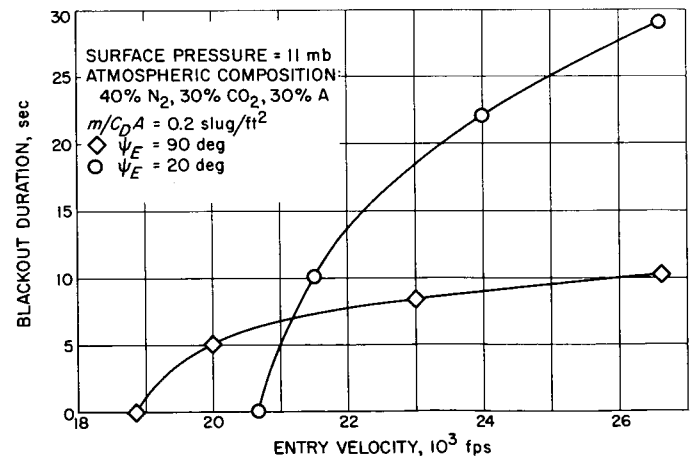


Fig. 13. Blackout duration versus entry velocity

The effects of variation in scale height on electron concentration can be shown by fixing the ratio of the local velocity on the trajectory to the entry velocity. From Eq. (11), this condition, in turn, determines a certain

absolute pressure in the atmosphere. The local atmospheric pressure is related to scale height and atmospheric density by

$$P = \frac{g_m \rho}{\beta} \quad (21)$$

where β is expressed in ft^{-1} . Therefore, if the scale height changes by a factor of three, the local density changes by a factor of three for a fixed local pressure (local velocity to entry velocity ratio). Substitution of the density variation into Eq. (19) shows that the electron concentration in the wake varies by less than a factor of three. Therefore, so long as the scale height does not change by a factor of three or more, the shifting of the electron concentration profile can be employed with little error.

Since equilibrium conditions are always utilized to estimate the electron concentration in the stagnation region, some idea of the effect of changing the atmospheric composition on electron concentration can be obtained by considering the Saha equation (Ref. 11). This equation, which may be used to determine the equilibrium thermal ionization fraction for a particular species, has the form

$$\log_{10} \left(\frac{X_i^2}{1 - X_i^2} \right) P_T = - \frac{5,050 U_i}{T} + 2.5 \log_{10} (T) - 6.5 \quad (22)$$

If the fractional ionization is small and the various species are only singly ionized (as in the case of interest), the electron concentration in the stagnation region can be obtained by utilizing Eq. (22) and summing over all species. For entry velocities of interest, the stagnation temperature is approximately 7000°K . In this case, the electron concentration obtained by using model atmosphere 1 relative to that obtained by using model atmosphere 2 (92.5 percent N_2 , 7.5 percent CO_2) is

$$\frac{(n_{e,0})_1}{(n_{e,0})_2} = \frac{\sum_{\text{all species in 1}} \left(\frac{10^{-0.722 U_i + 3.1}}{P_{T,1}} \right)^{1/2}}{\sum_{\text{all species in 2}} \left(\frac{10^{-0.722 U_i + 3.1}}{P_{T,2}} \right)^{1/2}} \quad (23)$$

where the summation over all species refers to the species present in the stagnation region. However, for purposes of comparison, only those species that are present after the gas is completely dissociated are considered. Now if the scale heights in the two model atmospheres are approximately the same, the densities and velocities will be approximately the same at some corresponding altitudes (perhaps a higher or lower altitude in 2 compared to 1); thus the pressures in the stagnation region will be approximately the same. With these assumptions, it may be shown that the electron concentration in the nominal model atmosphere (40 percent N_2 , 30 percent CO_2 , 30 percent A) is approximately twice the electron concentration in model atmosphere 2 (92.5 percent N_2 , 7.5 percent CO_2). Doubling the amount of CO_2 in the atmosphere over the nominal amount would also approximately double the electron concentration. Although this calculation was limited to a stagnation-region temperature of 7000°K , a similar result was obtained for a 5000°K temperature in the stagnation region. Thus variations in atmospheric composition are second-order effects so long as there is some CO_2 present (carbon is the principal contributor of electrons). However, even should there be no CO_2 present, the electron concentration would be only a factor of four less than the electron concentration calculated for the nominal model atmosphere.

This study has been limited to an analysis of blunt bodies, since they appear to be more desirable for future soft-landing missions on the Martian surface; however, an analysis has also been performed to evaluate the communication blackout problem for high-ballistic-coefficient conical bodies. In this case, it appears that transmission through the wake of the body would be impossible if entry velocities of approximately 25,000 fps are utilized. Transmission transverse to the capsule roll axis is less difficult, but the results are quite sensitive to angle-of-attack oscillations and to the state of the boundary layer (whether laminar or turbulent). For a high-ballistic-coefficient body, the characteristic dimension is in centimeters (on the order of boundary-layer thickness); thus, for the same attenuation, much higher entry velocities can be utilized, provided that communication is transverse to the body roll axis.

VI. CAPSULE INSTRUMENTATION AS AN ENTRY FAILURE CONTINGENCY

Another aspect of capsule design associated with the blackout period is the possible failure of the capsule during the entry blackout period. If this were to occur, it would be desirable to have at least some information regarding the Martian atmosphere prior to blackout. Those characteristics that might be measured are the capsule deceleration and perhaps the surface temperature of the heat shield. As mentioned previously, the capsule deceleration may be expressed in the form of Eq. (13). Since the surface temperature of the capsule is dependent on the radiative and the convective heat-transfer rates in the stagnation region, it too can be considered to be a function of the free-stream density and the capsule velocity. As pointed out in Ref. 5, the deceleration and these two heating rates may be expressed as nondimensional fractions of their maximum values for various times

Table 1. Stagnation-region values of C , i , and j for a Mars-entry capsule

Characteristic	C^a	i	j
Deceleration, ft/sec ²	$\frac{1}{2} \Delta$	1.0	2.0
Convective heating, Btu/ft ² -sec	$2.91 \times 10^{-8} r^{-\frac{1}{2}}$	0.5	3.19
Radiative heating, Btu/ft ² -sec	$1.13 \times 10^{-12} r$	1.4	5.0
Electron concentration, electrons/cm ³	4.9×10^{-32}	0.95	11.8

^aConstant evaluated for density in slugs/ft³, for velocity in ft/sec, and for capsule nose radius in ft.

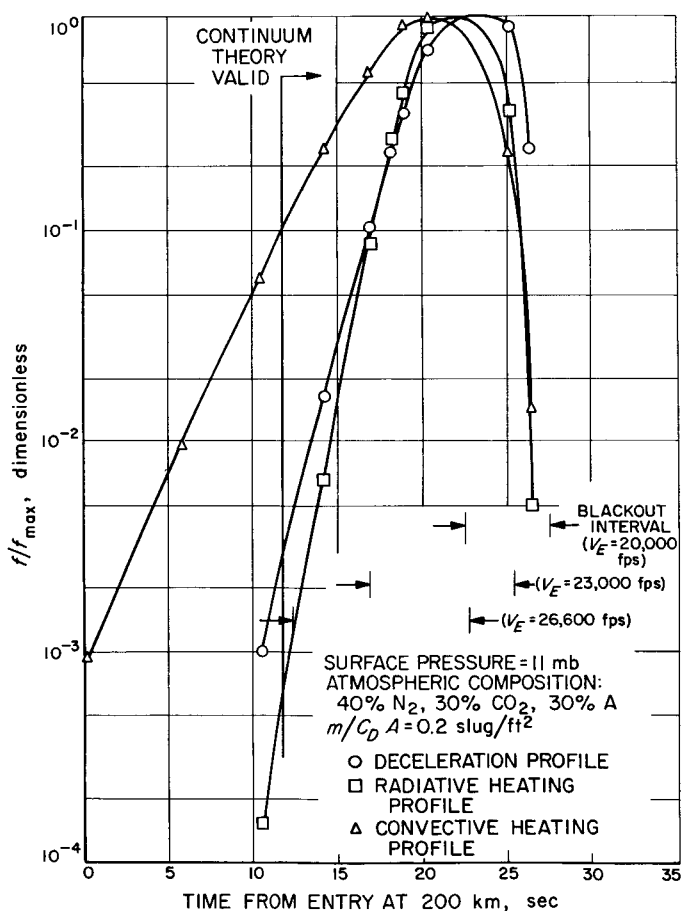


Fig. 14. Profiles for deceleration and for convective and radiative heat-transfer rates during entry for $\psi_E = 90$ deg

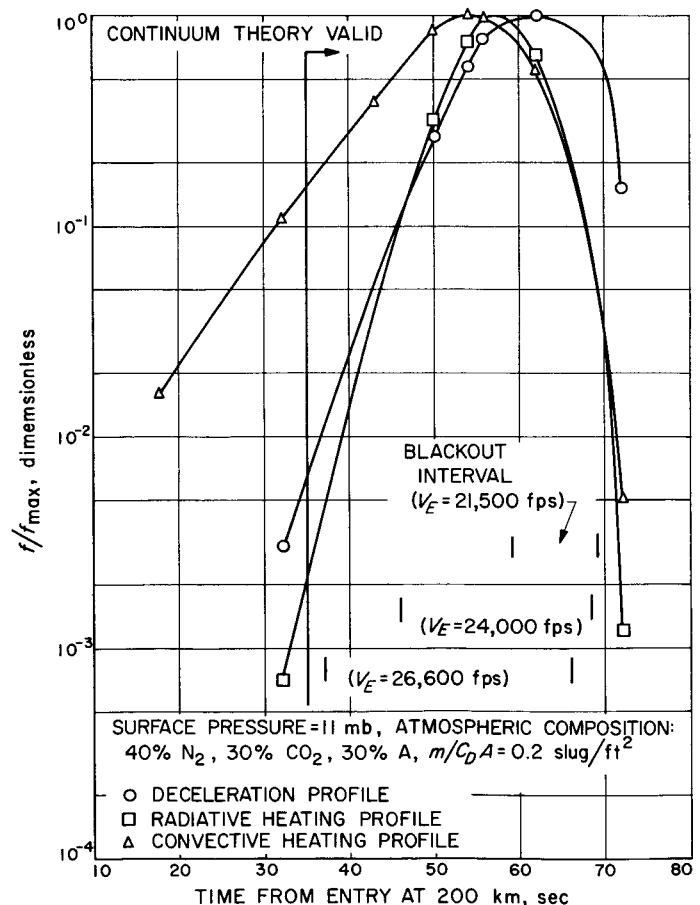


Fig. 15. Profiles for deceleration and for convective and radiative heat-transfer rates during entry for $\psi_E = 20$ deg

during entry. These fractions are dependent on the atmospheric composition, the capsule characteristics, and the entry angle, as well as on their relationship to density and velocity. The stagnation-region values of the coefficient and the exponents for the various parameters are given in Table 1 for a Mars entry.

Using the equations developed in Ref. 5,

$$\frac{F}{F_{\max}} = \left(\frac{x}{i}\right)^i \exp [i - x] \quad (24)$$

where

$$x = \frac{jP_{\infty}}{2\Delta \sin \psi_E} \quad (25)$$

the profiles for deceleration and for convective and radiative heat-transfer rates during entry may be determined.

These are presented in Fig. 14 and 15 for entry angles of 90 and 20 deg, respectively. Superimposed on these graphs is the potential blackout-time interval determined above. The results show that the time available for pre-blackout measurements is very dependent on the entry velocity. If the entry velocity is 26,600 fps, there is approximately no time available from the inception of the continuum flow regime to the onset of blackout. For lower velocities, there appears to be sufficient time for deceleration and temperature measurements prior to blackout. These measurements would be useful in determining indirectly the properties of the Martian atmosphere, should the capsule fail to endure the entry or should the low-speed experiments fail to provide data. Based on the potential reward of preblackout measurements, it appears that further study is warranted to investigate the possibility of instrumenting the capsule to make these engineering measurements.

VII. OTHER CONSIDERATIONS IN THE FLOW FIELD AND METHODS OF ELIMINATING BLACKOUT

In the previous discussion, it has been shown that the electron concentration can be considered to be frozen with the same total number of electrons as are present in the stagnation region as the gas flows around the entry capsule. An alternate way of analyzing the electron flow is to consider the reactions that will alter the electron concentration. There are two principal mechanisms for eliminating electrons from the flow field: (1) recombination with positive ions and (2) attachment to neutral atoms. The rate of electron depletion by recombination is given by

$$\frac{dn_e}{dt} = -n_e \sum_{i=1}^I n_i^+ \alpha_i \quad (26)$$

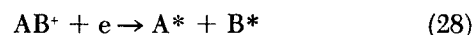
where the recombination coefficient α , as given in Ref. 12, is

$$\alpha_i = \bar{v}_e [Q_r(\bar{v}_e)]_i \quad (27)$$

and $Q_r(\bar{v})$ is the cross section for any particular mode of recombination evaluated at the mean electron speed.

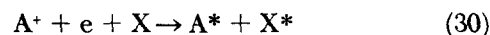
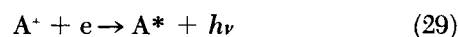
A consideration of the various modes of electron recombination indicates that the process with the largest cross section is dissociative recombination of electrons

with positively charged molecules. From Ref. 12, this reaction has the form



For the nominal Mars atmosphere, the concentrations of species in the stagnation region of the entry capsule that exhibit this large cross section (CO^+ , CO_2^+ , N_2^+ , etc.) are small compared to the concentration of electrons. Thus, even if this recombination rate were infinitely fast, the electron concentration would not be depleted significantly (less than 10 percent).

Most of the positive ions are atomic. The principal modes of their recombination with electrons are radiative recombination and three-body recombination in the presence of a neutral atom. From Ref. 12, these reactions have the form



The recombination coefficients for these modes, based on the calculated species concentrations in the stagnation region of the entry body, are $\alpha_R \approx 10^{-10}$ cm³/sec and

$\alpha_{th} \approx 10^{-11}$ cm³/sec, respectively. Since the recombination rates of atomic ions with electrons are approximately the same for all species and since the sum of atomic-ion concentrations is approximately equal to the electron concentration, Eq. (26) has the form

$$\frac{dn_e}{dt} = -n_e^2 (\alpha_R + \alpha_{th}) \quad (31)$$

Integrating,

$$\left(\frac{1}{n_{e,w}} - \frac{1}{n_{e,0}} \right) = (\alpha_R + \alpha_{th}) \Delta t_{res} \quad (32)$$

The time interval available for recombination is the residence time of the species from the stagnation region to the wake. The residence time, as discussed previously, is simply the length of the capsule divided by the capsule velocity:

$$\Delta t_{res} = -\frac{l_{cap}}{V_{cap}} \quad (33)$$

For the entry body under study, $l_{cap} \approx 10$ ft. In Fig. 16 are shown the recombination effects on the electron concentration, assuming there is no expansion of the gas as

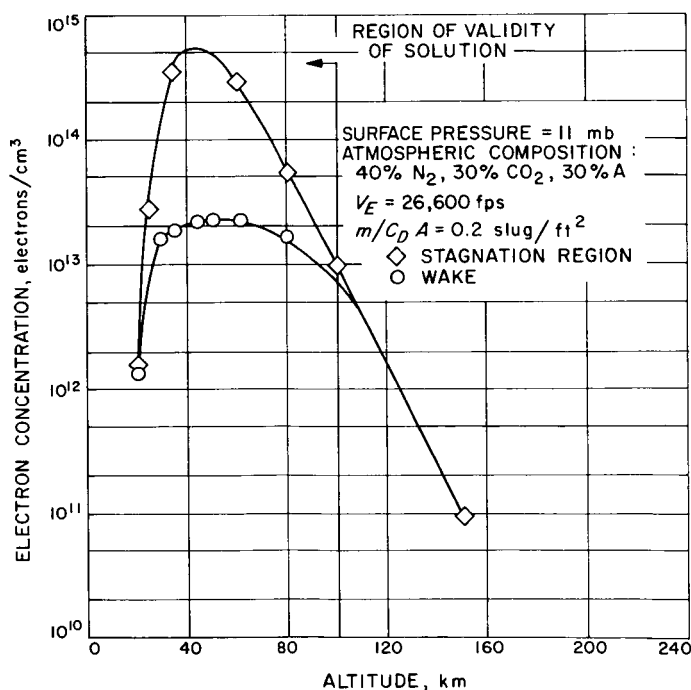


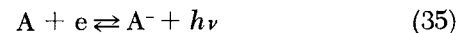
Fig. 16. Estimate of electron depletion resulting from recombination for $\psi_E = 90$ deg

it flows by the capsule. The results in Fig. 16 show that there is insufficient time for complete recombination as the gas flows around the capsule, even if the electron concentration has its stagnation-region value. The degree of recombination indicated in Fig. 16 is, therefore, overestimated, since the electron and ion concentrations actually decrease as the flow expands around the capsule. Thus, these results also indicate that the flow of electrons is nearly frozen.

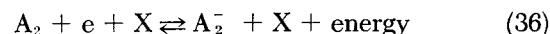
Another mechanism for depleting the electron concentration is the attachment to neutral atoms or molecules. In this case, the rate of electron depletion is given by Eq. (12):

$$\frac{dn_e}{dt} = -n_e \bar{v}_e \sum_{i=1}^I n_i^n Q_{att,i}(\bar{v}) \quad (34)$$

From Ref. 13 and 14, the primary attachment mechanisms for low-energy electrons (< 1 ev) are radiative attachment



three-body attachment



and dissociative attachment



Attachment cross section data for many of the species of interest during the Mars entry have been determined; in most cases, however, the data correspond to electron energies above 2 ev and are observed in low-temperature plasmas. These results indicate that the three-body attachment cross section is much greater than the dissociative cross section for electron energies of 1 ev at low gas temperatures; however, the inverse collisional detachment process becomes dominant at high gas temperatures (as in the stagnation region of the entry body).

Experimental results have been extrapolated in order to estimate the attachment cross sections of dry air (Ref. 15), water vapor (Ref. 16), oxygen (Ref. 17), carbon dioxide (Ref. 18), and carbon monoxide (Ref. 19). All of this information indicates that the total attachment cross section for electrons with energies in the range from 0.5 to 1.0 ev is on the order of 10^{-22} to 10^{-20} cm². There are fewer cross section data available for electron attachment to neutral atoms; however, the results for O and H

indicate that this attachment section is also on the order of 10^{-22} cm².

By using the cross section data given above for all neutral molecules and atoms, the depletion of electrons by attachment was determined to be negligible during the flow over the body. Since it is expected that values of the cross sections utilized were greater than would actually pertain to the composition of the flow, it appears that electron attachment will not be important in determining the wake electron concentration.

In the process of obtaining electron-attachment cross section data for the species present in the flow, it became apparent that halogenated molecules exhibit a very strong electron affinity. It would appear, therefore, that the injection of halogenated molecules into the flow could substantially reduce the free electron concentration and thereby potentially eliminate the blackout problem. The injection of fluids into the wake of an entry body has previously been examined at Langley Research Center (LRC) (Ref. 20). However, Ref. 20 states that the mechanism of electron depletion from injection of water or Freon into an ionized gas is not understood, although their experiments indicate that the process is not simply thermal quenching. Although the details of the LRC experimental work were not available to the author, an approximate analysis using electron-attachment data for water and Freon allowed the author to bracket the flow rates actually employed in the LRC experiments. Although these calculations are not conclusive, they do indicate that the most probable mechanism is electron attachment. Since there is a great deal of interest in eliminating communication blackout during the Mars entry and, in addition, for manned Earth entry, an approximate analysis based on the electron attachment process was performed for the Mars-entry flow conditions.

The cross section data of Buchel'nikova (Ref. 21) for SF₆ (sulfur hexafluoride), CCl₄ (carbon tetrachloride), CCl₂F₂ (Freon), BCl₃, HBr, HCl, H₂O, and O₂ were examined to determine the best fluid for injection into the flow. Sulfur hexafluoride exhibits the largest cross section, 5.7×10^{-16} cm²; however, the first resonance occurs at a very low energy (< 0.02 eV) and has a narrow half width. The attachment cross section for CCl₄ exhibits resonance values of 1.3×10^{-16} cm² and 1.0×10^{-16} cm² for electron energies of 0.02 and 0.6 eV, respectively. The expected average energy of the electrons in the wake is approximately 0.6 to 0.7 eV; thus CCl₄ was chosen in order to estimate the effect of injectant on the electron concentration.

In order to obtain at least the order of magnitude of required flow rates, the following assumptions are made:

1. The injectant is uniformly distributed over the capsule wake instantaneously and is not dissociated.
2. The concentration of injectant in the wake must be much greater (at least a factor of ten) than the electron concentration in the wake so the depletion of injectant is negligible.
3. The volume per unit time that must be filled is determined by the frontal area of the capsule times the capsule velocity.
4. All electrons are produced in the stagnation region and there is no *depletion* except by attachment to the injected molecules, although the concentration decreases because of the expansion from the stagnation region to the wake.
5. The electron concentration in the wake that must be quenched is given by the frozen-flow or the semi-frozen-flow expansion (see Fig. 5).

With these assumptions, Eq. (34) may be integrated to give

$$n_{inj} = \frac{1}{Q_{att, inj} (\bar{v}_e) \bar{v}_e \Delta t_{att}} \ln \frac{n_{e,w}^0}{n_{e,w}^c} \quad (38)$$

The time interval available for the reaction is approximately

$$\Delta t_{att} \simeq \frac{z_{att}}{V_{cap}} \quad (39)$$

where z_{att} is a characteristic length. This length is determined by the injection location, the mixing length of the injectant, and the antenna location. For the *Mariner* capsule, this characteristic length must be on the order of 1 ft. Using assumption 5, and recalling that the critical electron concentration is 10^{11} electrons/cm³ for S-band transmission, the concentration of injectant necessary to deplete the electron concentration can be *estimated*. The instantaneous flow rate of injectant can then be calculated if it is assumed that the flow must completely fill the volume swept out by the capsule frontal area. Then,

$$\dot{w}_{inj} = 62.4 \frac{n_{inj} (MW_{inj})}{N_{R_0}} V_{cap} A_{cap} \quad (40)$$

The estimated flow rate of CCl₄ required to reduce the electron concentration below the critical value is given in Fig. 17 for a Mars-entry velocity of 26,600 fps and a

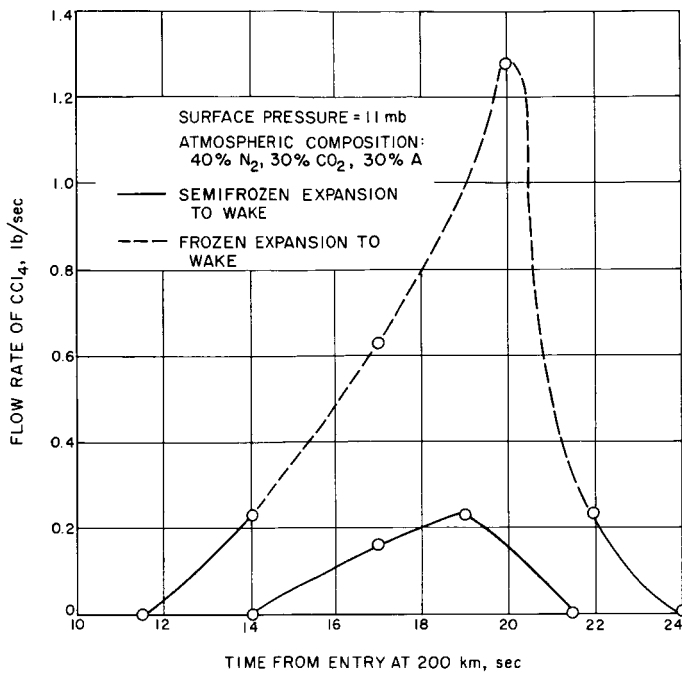


Fig. 17. Estimated flow rate of CCl_4 necessary to eliminate blackout during Mars entry for $V_E = 26,600$ fps, $m/C_D A = 0.2$ slug/ft², and $\psi_E = 90$ deg

maximum capsule diameter of 10 ft. The estimated total required amount of CCl_4 (obtained by integrating the graphical results in Fig. 17) is 1 lb, assuming a semi-frozen-flow expansion, and approximately 6 lb, assuming a completely-frozen-flow expansion.

It should be realized that these estimates of the weight of injectant are dependent on the gross assumptions made in the analysis; however, the required total amount of injectant appears to be small enough to justify further investigation of this technique. This effort would require laboratory testing to determine the effectiveness of the injectant in quenching the free electron concentration.

The most important assumption that was made in the preceding analysis is that CCl_4 is not dissociated by mechanisms other than the electron attachment mechanism. The following discussion is an analytical examination of this assumption. The principal competing mechanism for the dissociation of CCl_4 is through molecular collisions. From Ref. 22, the total number of collisions of the injectant per unit volume in the gas is given by

$$n_{\text{inj}} v_i^{\text{inj}} = \pi n_{\text{inj}} \sum_{i=1}^n \bar{v}_i \sigma_{\text{inj}, i} n_i \quad (41)$$

However, only a portion of these molecular collisions effectively dissociates the injectant (CCl_4). If it is assumed that all atomic and molecular species are equally effective in producing dissociations, the rate of molecular dissociation is given by

$$\frac{dn_{\text{inj}}}{dt} = -q n_{\text{inj}} v_i^{\text{inj}} \quad (42)$$

where q is the collision efficiency or ratio of the effective number of gas kinetic collisions leading to dissociation to the total number of collisions. Now the desired reaction (electron attachment) also depletes the amount of injectant. Including this effect on a collisional basis, the total rate of depletion of injectant is

$$\frac{dn_{\text{inj}}}{dt} = -n_{\text{inj}} (q v_i^{\text{inj}} + v_e^{\text{inj}}) \quad (43)$$

In order to obtain an estimate of the relative importance of molecular dissociation of the injected fluid owing to gas atom and molecular impact rather than electron impact, Eq. (43) may be rearranged in the form

$$\frac{dn_{\text{inj}}}{dt} = -n_{\text{inj}} v_e^{\text{inj}} \left(1 + \frac{q v_i^{\text{inj}}}{v_e^{\text{inj}}} \right) \quad (44)$$

Now the relative importance of the two effects can be obtained by comparing the magnitude of $(q v_i^{\text{inj}} / v_e^{\text{inj}})$ with 1. By definition,

$$\frac{q v_i^{\text{inj}}}{v_e^{\text{inj}}} = \frac{q \pi \sum_{i=1}^I \bar{v}_i \sigma_{\text{inj}, i}^2 n_i}{n_e \bar{v}_e Q_e^{\text{inj}}} \quad (45)$$

From molecular collision theory,

$$q = p e^{-E/RT} \quad (46)$$

where p is the steric factor (a measure of the number of collisions that have the proper orientation to produce dissociation) and E is the activation energy required for the reaction to take place. The interaction diameter is given by

$$\sigma_{\text{inj}, i} = \sigma_{\text{inj}} + \sigma_i \quad (47)$$

For species present in the vicinity of the Mars-entry capsule, the individual collision diameters are approximately equal and have a value of 3.6×10^{-8} cm. The experimental value of the collision area for CCl_4 is 22.0 \AA^2 (Ref. 23), which yields a collision diameter of 5.3×10^{-8} cm. The theoretical value of the collision diameter of CCl_4 is 5.4×10^{-8} cm (Ref. 24), which is in excellent agreement with the measured value. Thus, the interaction diameter is $2.0 \times 10^{-15} \text{ cm}^2$.

A mean molecular weight of 20 is adopted for the gas in the vicinity of the entry capsule for the 40 percent N_2 , 30 percent CO_2 , 30 percent A atmospheric model. If it is assumed that the electrons and gas atoms have the same kinetic temperature,

$$\frac{\bar{v}_i}{\bar{v}_e} = \left[\frac{m_e N_{R0}}{(MW)_g} \right]^{1/2} \approx \frac{1}{200} \quad (48)$$

The attachment cross section for electrons to carbon tetrachloride is 10^{-16} cm^2 . Thus,

$$\left(\frac{q v_i^{inj}}{v_e^{inj}} \right) = 0.3 p e^{-E/RT} \left(\frac{n_T}{n_e} \right) \quad (49)$$

From Semonov (Ref. 25), the experimental value of the activation energy for the decomposition of CCl_4 , as measured by Shilov, is 55.1 kcal/mole. However, Semenov points out that the expected value should be nearer the carbon-chlorine bond energy of 68–70 kcal/mole. A value of 68 kcal/mole is used in this analysis.

The remaining factor to be determined is the steric factor. The maximum value of this factor is 1; for complicated molecules, however, it is more likely to have a value on the order of 0.1 or less (Ref. 22). For conservatism, a value of $p = 0.25$ is adopted in this analysis.

An evaluation of Eq. (49) for a gas kinetic temperature of 7000°K yields

$$\left(\frac{q v_i^{inj}}{v_e^{inj}} \right) = 5 \times 10^{-4} \left(\frac{n_T}{n_e} \right) \quad (50)$$

The ratio given in Eq. (50) is shown in Fig. 18 as a function of altitude for a 90-deg Mars-entry trajectory and an entry velocity of 26,600 fps. It may be seen that the dissociation rate owing to molecular impact is less than the dissociation rate owing to electron attachment until the vehicle reaches an altitude of approximately 35 km. Below this altitude, molecular collisions will dominate the CCl_4 dissociation. However, even though the CCl_4 may be partially dissociated, the dissociated species, that is, CCl_3 , CCl_2 , will attach electrons and may, in fact, have a higher electron affinity than CCl_4 . In any case, for altitudes of less than 35 km, the gas will nearly be in equilibrium and it is expected that the electron concentration in the wake will be less than the

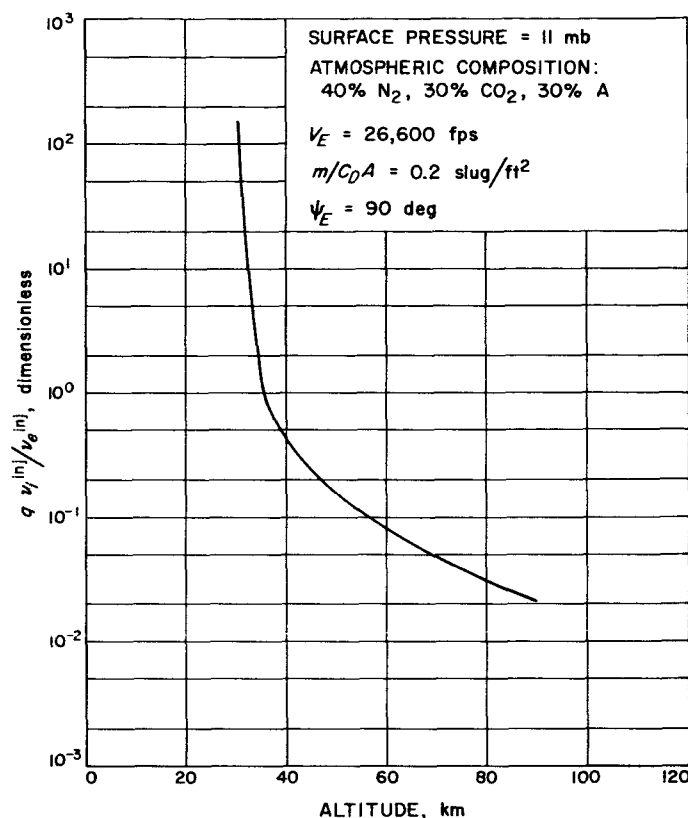


Fig. 18. Relative importance of atomic and electron collisions in CCl_4 dissociation

critical value. Thus it appears that CCl_4 will be effective in reducing the free electron concentration over the range of altitudes in the Martian atmosphere where blackout is expected.

In summary, it appears that injection of carbon tetrachloride into the wake of the Mars-entry capsule may eliminate communication blackout at S-band frequencies for moderate injected weights. The primary mechanism for quenching the free electron concentration is through dissociative attachment to carbon tetrachloride. Although other effects will occur as the carbon tetrachloride comes into equilibrium with the hot gas, it appears that the nonequilibrium electron attachment in the vicinity of the vehicle is important in obtaining continuous transmission capability. However, the effectiveness of this mechanism over the entire range of conditions to be encountered in the Mars entry must be assessed experimentally.

VIII. CONCLUSIONS

The analysis indicates that communication from a low-ballistic-coefficient capsule will be interrupted during entry into the Mars atmosphere because of ionization in the vicinity of the entry body for entry velocities greater than 19,000–20,000 fps. Since the anticipated entry velocities for Mars-entry missions in 1966 and 1969 are significantly greater than this range, preventive methods must be employed if continuous communication with the

capsule is necessary. The most straightforward solution is the use of a retro braking rocket to reduce the capsule velocity prior to entry.

Another interesting solution is the injection of a high-electron-affinity fluid such as carbon tetrachloride into the wake of the entry body to reduce the free electron concentration (and signal attenuation) to an acceptable level.

NOMENCLATURE

A	frontal area, ft ²	N_{R_0}	Avogadro's number = 6.023×10^{23} molecules/mole
C	constant (dimensions depend on the characteristic considered)	n	species concentration, particles/cm ³
E	activation energy, cal/mole	P	pressure in Martian atmosphere, lb/ft ²
E_0/E	fractional energy transmitted through the plasma, dimensionless	p	steric factor, dimensionless
e	electron charge = 4.8×10^{-10} statcoulombs	Q	interaction cross section, cm ²
F	arbitrary function (dimensions depend upon the characteristic considered)	q	collision efficiency, dimensionless
f	transmission frequency, cycles/sec	R	universal gas constant = 1.98 cal/g-mole-°K
g_m	acceleration of gravity at the surface of Mars = 12.3 ft/sec ²	r	capsule nose radius, ft
H	absolute gas enthalpy, cal/g	S	absolute gas entropy, cal/g-°K
h	altitude, km	T	temperature, °K
i	exponent of the density term in Eq. (14)	t	time, sec
j	exponent of the velocity term in Eq. (14)	U	ionization potential, ev
k	Boltzmann's constant = 1.38×10^{-16} erg/(molecule-°K)	u	dummy variable of integration
k'	extinction coefficient, dimensionless	V	velocity, ft/sec
l	characteristic length of entry body, ft	\bar{v}	mean speed, cm/sec
M	Mach number, dimensionless	\dot{w}	flow rate, lb/sec
MW	cold-gas molecular weight, g/g-mole	X	fractional ionization, dimensionless
m	species mass, g	x	dimensionless parameter
		Z	ionic charge, dimensionless
		z	plasma thickness, cm
		α	recombination coefficient, cm ³ /sec
		β	scale height, km ⁻¹
		γ	isentropic expansion coefficient, dimensionless

NOMENCLATURE (Cont'd)

Δ	ballistic coefficient, slugs/ft ²
ϵ_0	permittivity of free space = $(1/4\pi)$ statcoulombs ² /dyne-cm ²
ζ	argument of exponential integral
κ	propagation constant, cm ⁻¹
λ	wavelength of transmitted signal, cm
ν	collision frequency, collisions/sec
ρ	density of atmosphere, slugs/ft ³
σ	collision diameter, cm
ψ	angle of velocity vector with respect to local horizontal, deg
ω	angular frequency, rad/sec

Subscripts

att	attachment
c	collision
cap	capsule
cr	critical
E	entry
e	electron
g	gas
i	i-th species
inj	injectant
j	j-th species
max	maximum

p	plasma
R	radiative recombination
r	recombination
res	residence
s	surface
T	total
t	arbitrary time after entry
tb	three-body recombination
w	wake
λ	wavelength
0	stagnation region
1	atmospheric model 1 (nominal atmosphere: 40% N ₂ , 30% CO ₂ , 30% A)
2	atmospheric model 2 (92.5% N ₂ , 7.5% CO ₂)
∞	free stream

Superscripts

cr	critical value
i	ion
inj	injectant (carbon tetrachloride)
n	neutral
V_E	evaluated at entry conditions
0	value without injectant
26,600	evaluated for an entry velocity of 26,600 fps
—	average value

REFERENCES

1. Glasstone, S., and Lovberg, R. A., *Controlled Thermonuclear Reactions*, D. Van Nostrand, Inc., Princeton, New Jersey, 1960.
2. Rose, D. J., and Clark, M., Jr., *Plasma and Controlled Fusion*, The M. I. T. Press, Massachusetts Institute of Technology and John Wiley & Sons, Inc., New York, 1961.
3. Lin, S. C., *A Rough Estimate of the Attenuation of Telemetry Signals Through the Ionized Gas Envelope Around a Typical Re-entry Missile*, Report No. 74, Avco Corporation, Avco-Everett Research Laboratory, Everett, Massachusetts, February 1956.

REFERENCES (Cont'd)

4. Kaplan, L. D., Munch, G., and Spinrad, H., "An Analysis of the Spectrum of Mars," *The Astrophysical Journal*, Vol. 139, No. 1, 1964.
5. Ambrosio, A., "A General Atmospheric Entry Function and Its Characteristics," *ARS Journal*, Vol. 32, No. 6, June 1962, pp. 906-910.
6. Spiegel, J., "Effects of Mars Atmospheric Uncertainties on Entry Vehicle Design," *Aerospace Engineering*, Vol. 21, No. 12, December 1962, pp. 62-63, 103-107.
7. Hayes, W. D., and Probstein, R. F., *Hypersonic Flow Theory*, Academic Press Inc., New York, 1958.
8. Bray, K. N. C., "Simplified Sudden-Freezing Analysis for Nonequilibrium Nozzle Flows," *ARS Journal*, Vol. 31, No. 6, June 1961, pp. 831-834.
9. Fay, J. A., and Kemp, N. H., "Theory of Stagnation Point Heat Transfer in a Partially Ionized Diatomic Gas," (Avco Corporation, Avco-Everett Research Laboratory, Everett, Massachusetts), Paper 63-60, Institute of the Aerospace Sciences, Thirty-first Annual Meeting, New York, New York, January 21-23, 1963.
10. Wu, C.-S., *Some Remarks on the Assumption of Isotropy in Magnetoplasmdynamics*, Section Report No. 22-8, Jet Propulsion Laboratory, Pasadena, California, October 28, 1959.
11. Cobine, J. D., *Gaseous Conductors*, Dover Publications, Inc., New York, 1958.
12. Massey, H. S. W., and Burhop, E. H. S., *Electronic and Ionic Impact Phenomena*, Oxford University Press, London, 1952.
13. *Atomic and Molecular Processes*, ed. by D. R. Bates, Academic Press, Inc., New York, 1962.
14. Biondi, M. A., "Atomic Collisions Involving Low-Energy Electrons and Ions," *Advances in Electronics and Electron Physics*, Vol. 18, ed. by L. Marton, Academic Press Inc., New York, 1963, pp. 67-165.
15. Prasad, A. N., "Measurement of Ionization and Attachment Coefficients in Dry Air in Uniform Fields and the Mechanism of Breakdown," *Proceedings of the Physical Society*, Vol. 74, 1959, p. 33.
16. Prasad, A. N., and Craggs, J. D., "Measurement of Ionization and Attachment Coefficients in Humid Air in Uniform Fields and the Mechanism of Breakdown," *Proceedings of the Physical Society*, Vol. 76, 1960, pp. 223-232.
17. Prasad, A. N., and Craggs, J. D., "Measurement of Townsend's Ionization Coefficients and Attachment Coefficients in Oxygen," *Proceedings of the Physical Society*, Vol. 77, 1961, pp. 385-398.
18. Bhalla, M. S., and Craggs, J. D., "Measurement of Ionization and Attachment Coefficients in Carbon Dioxide in Uniform Fields," *Proceedings of the Physical Society*, Vol. 76, 1960, pp. 369-377.
19. Bhalla, M. S., and Craggs, J. D., "Measurement of Ionization and Attachment Coefficients in Carbon Monoxide in Uniform Fields," *Proceedings of the Physical Society*, Vol. 78, 1961, pp. 438-447.

REFERENCES (Cont'd)

20. Huber, Paul, "Consideration of the Communications Loss During Planetary Atmospheric Entry," Manned Planetary Mission Technology Conference, Lewis Research Center, Cleveland, Ohio, May 21-23, 1963; printed as NASA TMX-50120, July 1963. CONFIDENTIAL.
21. Buchel'nikova, I. S., "Cross Sections for the Capture of Slow Electrons by O₂ and H₂O Molecules and Molecules of Halogen Compounds," *Soviet Physics JETP*, Vol. 35 (8), No. 5, May 1959, pp. 783-791.
22. Frost, A. A., and Pearson, R. G., *Kinetics and Mechanism, a Study of Homogeneous Chemical Reactions*, 2nd ed., John Wiley & Sons, Inc., New York, 1961.
23. Sperry, E. H., and Mack, E., Jr., "The Collision Area of the Gaseous Carbon Tetrachloride Molecule," *The Journal of the American Chemical Society*, Vol. LIV, January-April, 1932, pp. 904-907.
24. Fogg, P. G. T., Hanks, P. A., and Lambert, J. D., "Ultrasonic Dispersion in Halomethane Vapours," *Proceedings of the Royal Society (London)*, Series A: Mathematical and Physical Sciences, Vol. 219, October 1953, pp. 490-499.
25. Semenov, N. N., *Some Problems of Chemical Kinetics and Reactivity*, Vol. 1, Trans. by J. E. S. Bradley, Pergamon Press, Inc., New York, 1958.

BIBLIOGRAPHY

1. Barthel, J. R., *A Note on Some Investigations of Re-entry Wakes*, Report Ph-119-M, Physics Section, General Dynamics/Convair, San Diego, California, April 26, 1961.
2. Browne, W. G., *Thermodynamic Properties of Some Atoms and Atomic Ions*, Engineering Physics Technical Memorandum No. 2, General Electric Co., Missile and Space Division, Valley Forge Space Technology Center, Philadelphia, Pennsylvania (no date).
3. Browne, W. G., *Thermodynamic Properties of Some Diatomic and Linear Polyatomic Molecules*, Engineering Physics Technical Memorandum No. 3, General Electric Co., Missile and Space Division, Valley Forge Space Technology Center, Philadelphia, Pennsylvania (no date).
4. Browne, W. G., *Comparison of Thermal Functions Generated for Species in the High Temperature Air System With Literature Values*, Advanced Aerospace Physics Test Memorandum No. 10, General Electric Co., Missile and Space Division, Valley Forge Space Technology Center, Philadelphia, Pennsylvania, May 28, 1962.
5. Capiiaux, R., and Karchman, L., "Flow Past Slender Blunt Bodies; A Review and Extension," IAS Paper 61-210-1904, National Institute of Aerospace Sciences/American Rocket Society Meeting, Los Angeles, California, June 13-16, 1961.

BIBLIOGRAPHY (Cont'd)

6. Coleman, E. R., and Doody, P. J., *On Chemical Processes in Hypersonic Shock Layers*, R-BSR-509, The Bendix Corporation, Systems Division, Ann Arbor, Michigan, March 1961.
7. Homic, S. G., and Phillips, R. L., "Communicating With the Hypersonic Vehicle," *Astronautics*, Vol. 4, No. 3, March 1959, pp. 36-37, 92, 94, 96, 98.
8. Howe, J. T., and Vregas, J. R., "The Dissociative Relaxation of CO₂ Behind Normal Shock Waves," 9th AAS Meeting, June 15-17, 1963.
9. James, C. S., "Experimental Study of Radiative Transport From Hot Gasses Simulating in Composition the Atmospheres of Mars and Venus," AIAA Conference on Physics of Entry into Planetary Atmosphere, Massachusetts Institute of Technology, Cambridge, Massachusetts, August 26-28, 1963.
10. Rotman, W., and Meltz, G., *Experimental Investigation of the Electromagnetic Effects of Re-entry*, AFCRL 87, Air Force Department, Air Research and Development Command, Cambridge Research Laboratories, March 1961.
11. Rudin, M., and Ragent, B., *High Temperature Thermodynamic Properties of Selected Gases; A Review*, Report No. 69, Itek Corporation, Vidya Division, Palo Alto, California, March 10, 1962.
12. Scala, S. M., *The Hypersonic Environment; Heat Transfer in Multicomponent Gases*, Report No. R 625 D 987, General Electric Co., Missile and Space Division, Space Sciences Laboratory, Philadelphia, Pennsylvania, December 1962.
13. White, J. R., "Communication During Re-entry Blackout," ARS 14th Annual Meeting, Washington, D. C., November 16-20, 1959.
14. Whittliff, C. E., and Wilson, M. R., *Low Density Stagnation-Point Heat Transfer in Hypersonic Air Flow*, ORL Technical Report No. 60-333, Cornell Aeronautical Laboratory, Inc., Buffalo, New York, February 1961.
15. Yakura, J. K., "A Theory of Entropy Layers and Nose Bluntness in Hypersonic Flow," ARS Paper-1983-61, American Rocket Society, International Hypersonics Conference, Massachusetts Institute of Technology, Cambridge, Massachusetts, August 16-18, 1961.